Jpn. J. Appl. Phys. Vol. 38 (1999) pp. 3403–3408
Part 1, No. 5B, May 1999

In Vivo Measurement of Small Velocity Signals and Change in Thickness of the Heart Walls

Hiroshi KANAI[*1], Yoshiro KOIWA[*2], Yoshiko SAITO[*3], Ikuko SUSUKIDA[*4] and Motonao TANAKA[*5]
Graduate School of Engineering, Tohoku University, Sendai 980-8579, Japan

(Received November 27, 1998; accepted for publication January 18, 1999)

We have previously developed a new method for accurately tracking the movement of the heart wall based on both the phase and magnitude of the demodulated signals to determine the instantaneous position of an object. By this method, velocity signals of the heart wall with small amplitudes less than several micrometers on the motion resulting from a heartbeat can be accurately detected. Moreover, the method has been applied to multiple points preset in the heart wall along an ultrasonic beam so that the spatial distributions of the local change in thickness during one cardiac cycle is determined. In this paper, the method is applied to the free wall of the right ventricle (RV), the interventricular septum (IVS), and the posterior wall of the left ventricle (LV). From the relationships among the results for these parts of the heart, new findings which characterize the velocity signals and the change in thickness in each cardiac period are described. This method offers potential for quantitative myocardial diagnosis.

KEYWORDS: velocity signal measurement, local change in thickness, myocardial contraction/relaxation, myocardial motility, cardiac cycle

1. Introduction

In the free wall of the right ventricle (RV), the interventricular septum (IVS), and the posterior wall of the left ventricle (LV) shown in Fig. 1(a), thickening and thinning periodically occur during myocardial contraction and relaxation as illustrated in Figs. 1(b) and 1(c). This thickening and thinning at each local area in the heart wall corresponds to the regional myocardial motility, which originates from the sliding of the myosin and actin fibers. To noninvasively realize evaluation of this motility using ultrasound, it is necessary to *track* the instantaneous positions $x_A(t)$ and $x_B(t)$ of the two points A and B which are preset at the end-diastole along an ultrasonic beam in the heart wall. Then, the change in thickness, $\Delta h_{AB}(t)$, between these two points A and B from their thickness, h_0, at the end-diastole is obtained from the difference between $x_A(t)$ and $x_B(t)$ as illustrated in Fig. 1(c) if the ultrasonic beam is almost perpendicular to the wall during the cardiac cycle.[1,2] Such noninvasive measurement of the change in thickness of the regional area in the heart wall during each cardiac cycle provides essential tools for the diagnosis of heart diseases.

Though M-mode echocardiography offers an advantage in critically looking at the motion pattern of the LV, its spatial resolution along the ultrasonic beam is limited to a few wavelengths, namely, only up to 1 mm for ultrasound of 3 MHz because an M-mode image is displayed based on the amplitude of the reflected ultrasound. On the other hand, there have been numerous elaborate techniques proposed for noninvasive measurement of the velocity of the blood flow in the heart or the arteries based on the Doppler effect.[3] Moreover, several methods, including the phase-locked-loop (PLL) techniques, have been proposed to measure rough changes in the diameter of the arterial walls by tracking arterial wall displacement in real time.[4,5]

For the accurate detection of velocity signals, that is, the instantaneous movement on or in the heart wall, we have developed the following "*phased tracking method*".[2] This method has been confirmed by experiments using a water tank and has been applied to the *in vivo* detection of small velocity signals, with sufficient reproducibility, on the wall of the human heart.[2] The detected velocity signals show rapid motion including high frequency components with small amplitudes, which are difficult to recognize by M-mode echocardiography.

Moreover, the method has been applied to multiple points preset along an ultrasonic beam in the LV wall so that the instantaneous object positions, $\{x_i(t)\}$, and the velocity signals, $\{v(x_i; t)\}$, are obtained for these multiple points, $\{i\}$, in the LV wall.[1] From the results, by deleting the *parallel component*, the *thickness change components during myocardial contraction/relaxation* are detected. Then, their spatial distribution is obtained and is superimposed on the M-mode image using a color code.

Spectrum analysis was first applied to the resultant noninvasively detected signals to identify the frequency band for the components from 25 Hz to 90 Hz due to the myocardial thickening and thinning. Such analysis shows the novel possibility of diagnosis of the local myocardium.[1,2]

For such waveform analysis and/or spectrum analysis, however, it is significant to characterize each of six periods in one cardiac cycle using the results of the velocity signals and the change in thickness, which are measured by our method. For this purpose, in this study, the developed method was applied to the free wall of the RV, the IVS, and the posterior wall of the LV of a healthy young male volunteer and the IVS of a male patient with dilated-cardiomyopathy (DCM). From the relationship among the results for the three heart walls and the differences between the subjects, new findings which characterize the velocity signals and the change in thickness in each period during one cardiac cycle are described.

2. Principles of Measurement of Change in Thickness of the Wall

By referring to the M-mode image, which is reconstructed from the A/D converted data, we manually preset two points, A and B, in the heart wall or arterial wall along an ultrasonic

[*1]Graduate School of Engineering, Tohoku University, Sendai 980-8579, Japan. E-mail address: hkanai@ecei.tohoku.ac.jp
[*2]First Department of Internal Medicine, School of Medicine, Tohoku University, Sendai 980-8575, Japan.
[*3]Third Department of Internal Medicine, School of Medicine, Tohoku University, Sendai 980-8575, Japan.
[*4]Graduate School of Engineering, Tohoku University, Sendai 980-8579, Japan.
[*5]Tohoku Welfare Pension Hospital, Takasago 10, Fukumuro, Miyagino-ku, Sendai 983, Japan.

beam at a time t_0 of R-wave of the electrocardiogram (ECG) as illustrated in Fig. 1(b). We assume that both point A and point B have only a velocity component which is parallel to the direction of the beam if the direction and position of the ultrasonic beam are appropriately selected so as to be perpendicular to the wall during the cardiac cycle. The principle of the accurate detection of the change in thickness, $\Delta h_{AB}(t)$, between points A and B in the wall is briefly described as follows.[2)]

2.1 *For measurement of instantaneous movement $\Delta d_i(t)$ of object (i)*

RF pulses with an angular-frequency of $\omega_0 = 2\pi f_0$ are transmitted at a time interval of ΔT from an ultrasonic transducer. The ultrasonic pulse reflected by the object (i) is received by the same ultrasonic transducer. The output signal is amplified and quadrature-demodulation is applied to the signal. The resultant in-phase and quadrature signals for each transmitted pulse are simultaneously A/D converted at a sampling frequency of $1/T_S$, and these two signals are combined into a complex signal, $y(x;t)$, where $x(t)$ and its simple expression x denote the depth from the ultrasonic transducer. The instantaneous depth $x_i(t)$ of the object, (i), from the ultrasonic transducer is given by the product of the acoustic velocity, c_0, and the instantaneous period $\tau_i(t)$ required for one-way transmission from the ultrasonic transducer to the object, (i). The phase $\theta(x_i;t)$ of the signal $y(x_i;t)$ is given by the angular frequency ω_0 multiplied by twice the delay time $\tau_i(t)$. Thus, the phase difference $\Delta\theta(x_i;t)$ between the analytic signals $y(x_i;t)$ and $y(x_i;t+\Delta T)$ of the successively received signals in the interval ΔT is given by

$$\begin{aligned}\Delta\theta(x_i;t) &= \theta(x_i;t+\Delta T) - \theta(x_i;t)\\ &= 2\omega_0\{\tau_i(t+\Delta T) - \tau_i(t)\}\\ &= \frac{2\omega_0}{c_0}\Delta d_i(t),\end{aligned} \tag{1}$$

where $\Delta d_i(t) = x_i(t+\Delta T) - x_i(t)$ is the instantaneous movement of the object (i) in the period ΔT after a time t. Then, $\Delta d_i(t)$ is given from the measured data by

$$\Delta d_i(t) = c_0 \cdot \frac{\Delta\theta(x_i;t)}{2\omega_0}. \quad \text{(m)} \tag{2}$$

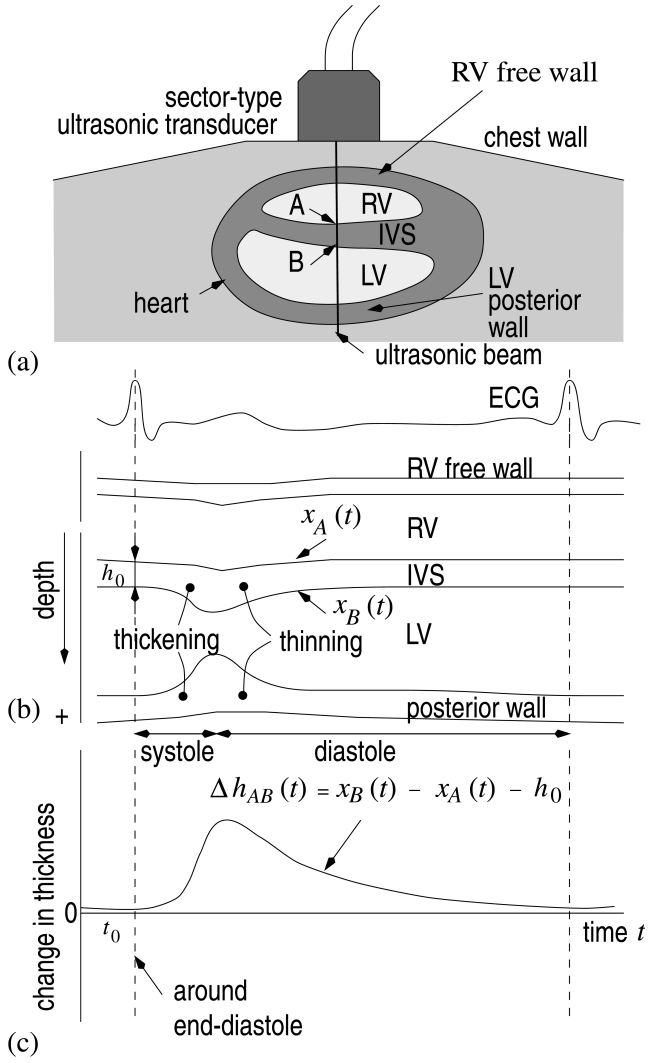

Fig. 1. An illustration explaining the procedure used to measure the change in thickness of (c) by tracking the movement $x_A(t)$ and $x_B(t)$ of points A and B preset in one of the three heart walls along the ultrasonic beam. (a) cross-sectional image, (b) ECG and the displacement, $x_A(t)$ and $x_B(t)$, superimposed on the M-mode image, (c) change in thickness, $\Delta h_{AB}(t)$.

2.2 *For accurate determination of the phase change $\Delta\theta(x_i;t)$*

Since it is essential to accurately determine the phase change $\Delta\theta(x_i;t)$ of eq. (2) during the period ΔT, the following complex correlation is introduced into the determination procedure of the instantaneous movement of the object position $x_i(t)$.[2)]

Since $y(x;t)$ and $y(x;t+\Delta T)$ are described by the damped sinusoidal signals, the standard cross-correlation procedure does not uniquely determine the optimum movement δ_x of $y(x;t+\Delta T)$ from $y(x;t)$ as theoretically described.[2)] To solve this problem, by restricting the magnitude of the average change $\beta(\delta_x;x_i;t)$ from $y(x;t)$ to $y(x+\delta_x;t+\Delta T)$ around $x_i(t)$ to one and replacing $\beta(\delta_x;x_i;t)$ by $\exp\{j\Delta\theta(\delta_x;x_i;t)\}$, we define the normalized mean squared difference, $\alpha(\Delta\theta;\delta_x)$, between $y(x_i+\delta_x;t+\Delta T)$ and $y(x_i;t)$. From the phase change $\widehat{\Delta\theta}(x_i;t)$ by which minimization of $\alpha(\Delta\theta;\delta_x)$ with respect to δ_x is achieved, the instantaneous movement of $\Delta d_i(t)$ in eq. (2) is given by

$$\widehat{\Delta d_i}(t) = c_0 \cdot \frac{\widehat{\Delta\theta}(x_i;t)}{2\omega_0}. \quad \text{(m)} \tag{3}$$

By dividing $\widehat{\Delta d_i}(t)$ by ΔT, the velocity signal is given as follows:

$$\widehat{v_i}(t) = \frac{\widehat{\Delta d_i}(t)}{\Delta T}. \quad \text{(m/s)} \tag{4}$$

The velocity signal and the spectrum will be effective in diagnosis of the local myocardium.[1)]

2.3 *For tracking of the object position $x_i(t)$*

The position $x_i(t)$ of the object (i) in the heart wall changes by more than 10 mm due to the heartbeat in one cardiac cycle. It is, therefore, necessary to track the instantaneous object position $x_i(t)$. For this purpose, by accumulating the estimate $\widehat{\Delta d_i}(t)$ of the instantaneous movement in eq. (3), the next object position $\widehat{x_i}(t+\Delta T)$ is estimated by

$$\widehat{x_i}(t+\Delta T) = \widehat{x_i}(t) + \widehat{\Delta d_i}(t). \quad \text{(m)} \tag{5}$$

Thus, the instantaneous movement $\widehat{\Delta d_i}(t)$ and the next object position $\widehat{x_i}(t + \Delta T)$ are simultaneously determined and are obtained as waveforms.

When the time interval, ΔT, of the transmission of the RF pulses is about 200 μs, the maximum value of the instantaneous movement $\Delta d(t)$ of an object in the heart wall is about 20 μm during the time interval ΔT. These values are much less than the wavelength of about 500 μm at 3 MHz. Since the quadrature-demodulated signals are A/D converted as a sampling interval, T_S, of 1 μs in this paper, the spatial resolution $\Delta x_S = T_S \times c_0/2$=750 μm in the direction of depth. However, the resultant estimate $\widehat{x_i}(t)$ of the next object position of eq. (5) in the above procedure is represented not by a discrete value which depends on the sampling interval T_S but by the continuous value which is determined from the phase difference $\widehat{\Delta\theta}(x_i; t)$. Thus, accurate tracking of the object is realized by this method and a small instantaneous movement of micron order is determined.

2.4 For measurement of change in thickness of the wall

Let us assume that the ultrasonic beam is almost perpendicular to the wall during one cardiac cycle and that the velocity direction of each point (i) in the wall is parallel to the direction of the ultrasonic beam. Thus, from the difference between the instantaneous object positions $x_i(t)$ and $x_{i+1}(t)$, the *thickness* of the local region, which is denoted by $h_i(t)$, is obtained by

$$\widehat{h_i}(t) = \widehat{x_{i+1}}(t) - \widehat{x_i}(t). \quad \text{(m)} \tag{6}$$

The change in thickness, $\Delta h_i(t)$, from the initial value $h_i(t_0)$ at time t_0 is obtained from the estimated velocity, $v_i(t)$ and $v_{i+1}(t)$, as follows:

$$\begin{aligned}\widehat{\Delta h_i}(t) &= \widehat{h_i}(t) - h_i(t_0) \\ &= \int_{t_0}^{t} \{\widehat{v_{i+1}}(t) - \widehat{v_i}(t)\}\mathrm{d}t, \quad \text{(m)}\end{aligned} \tag{7}$$

where $\Delta d_i(t) = v_i(t) \times \Delta T$. When the region between the ith and $(i + 1)$-th points becomes thicker at time t, $\Delta h_i(t) > 0$, while for the case when the region becomes thinner, $\Delta h_i(t) < 0$. However, $\Delta h_i(t)$ depends on the distance between $x_i(t)$ and $x_{i+1}(t)$. Thus, by dividing $\Delta h_i(t)$ by the distance $|x_{i+1}(t) - x_i(t)|$, the *normalized speed of the local change in thickness* which occurs in the assumed homogeneous myocardium between points (i) and $(i + 1)$, denoted by $S_i(t)$, is defined by

$$S_i(t) = \frac{\Delta h_i(t)}{|x_{i+1}(t) - x_i(t)|}. \quad \text{[(m/s)/m]} \tag{8}$$

The spatial distributions $\{S_i(t)\}$ of the normalized speed of the local change in thickness are color-coded and superimposed on the M-mode image. In our papers, *red* corresponds to thinning of the myocardium ($S_i(t) < 0$) and *blue* corresponds to thickening of the myocardium ($S_i(t) > 0$).

3. *In Vivo* Experimental Results for the Heart Walls

3.1 Explanation of the procedure of the proposed method

Firstly, the proposed method is applied to the detection of velocity signals on the free wall of the RV, the IVS, and the posterior wall of the LV of a healthy 24-year-old male volunteer. Figures 2(e-1), 2(e-2), and 2(e-3) show the B-mode images of these walls along the longitudinal axis, which were obtained by standard ultrasonic diagnostic equipment. Multiple points $\{i\}$ are set in each wall. Since the results obtained by the proposed method depend on the angle between the direction of the velocity vector and the ultrasonic beam, the direction of the ultrasonic beam passing through these walls is selected so that the beam is almost perpendicular to each wall, as shown in Figs. 2(e-1), 2(e-2), and 2(e-3), during the A/D conversion of several cardiac cycles. During the acquisition period, respiration is suspended.

Figures 2(a) and 2(b) show the ECG and the phonocardiogram (PCG), respectively. Before applying the method described in §2, by referring to the M-mode image, which was reconstructed from the magnitude of the digitized signal of the analytic signals, the positions $\{\widehat{x_i}(t_0)\}$ of the multiple points $\{i\}$ in each wall are manually preset using the workstation at even intervals of Δx_S=0.75 mm. The tracking results $\{\widehat{x_i}(t)\}$, estimated by eq. (5) of the points $\{i\}$, are superimposed on the M-mode image by white lines as shown in Figs. 2(d-1), 2(d-2), and 2(d-3).

Figures 2(c-1), 2(c-2), and 2(c-3) show the superimposed estimates of the velocity signals $\{\widehat{v}(x_i; t)\}$ of each heart beat on the tracked points $\{\widehat{x_i}(t)\}$ on the free wall of the RV, the IVS, and the posterior wall of the LV, respectively, during 6 heartbeats. The vertical axis of these figures is inverted so that the negative value of the velocity, which is shown above the baseline, corresponds to the situation in which the object moves in the direction of the ultrasonic transducer on the chest wall, which is more easily understood. The resultant velocity signals are sufficiently reproducible for six heartbeat periods.

For the first cardiac cycle, Figs. 2(d-1), 2(d-2), and 2(d-3) show the tracking results $\{\widehat{x_i}(t)\}$ of the multiple points $\{i\}$ by white lines and the normalized speed of the local change in thickness, $\{S_i(t)\}$, of eq. (8). The values $\{S_i(t)\}$ are color-coded according to the coloring scheme described in §2.4, and the results are superimposed on the M-mode image.

3.2 Discussion of the myocardial movement of the healthy subject

From the velocity signals and the change in thickness of Fig. 2, which are first obtained by the developed method, there are several new findings as follows, which cannot be recognized in the M-mode image of the previous standard echocardiography.

3.2.1 Atriosystolic phase

See period "A" in Figs. 2(c) and 2(d). In this period, just after the timing of the P-wave in the ECG, the blood flows into the ventricle from the atrium through atrioventricular valves. From the velocity signals in Figs. 2(c-2) and 2(c-3), the IVS and the posterior wall of the LV move so that the LV expands. For the free wall of the RV, there is a small velocity component in Fig. 2(c-1) causing the RV to expand. However, clear movement is not recognized for the free wall of the RV as shown in the M-mode image of Fig. 2(d-1).

In Figs. 2(d-1), 2(d-2), and 2(d-3), since there are red components in this atriosystolic phase, all three walls become thin. Also, such change in thickness cannot be recognized in the M-mode image.

3.2.2 Isovolumetric contraction period

See period "IC" in Figs. 2(c) and 2(d). In this period, the ventricles start to contract, but the blood still does not flow

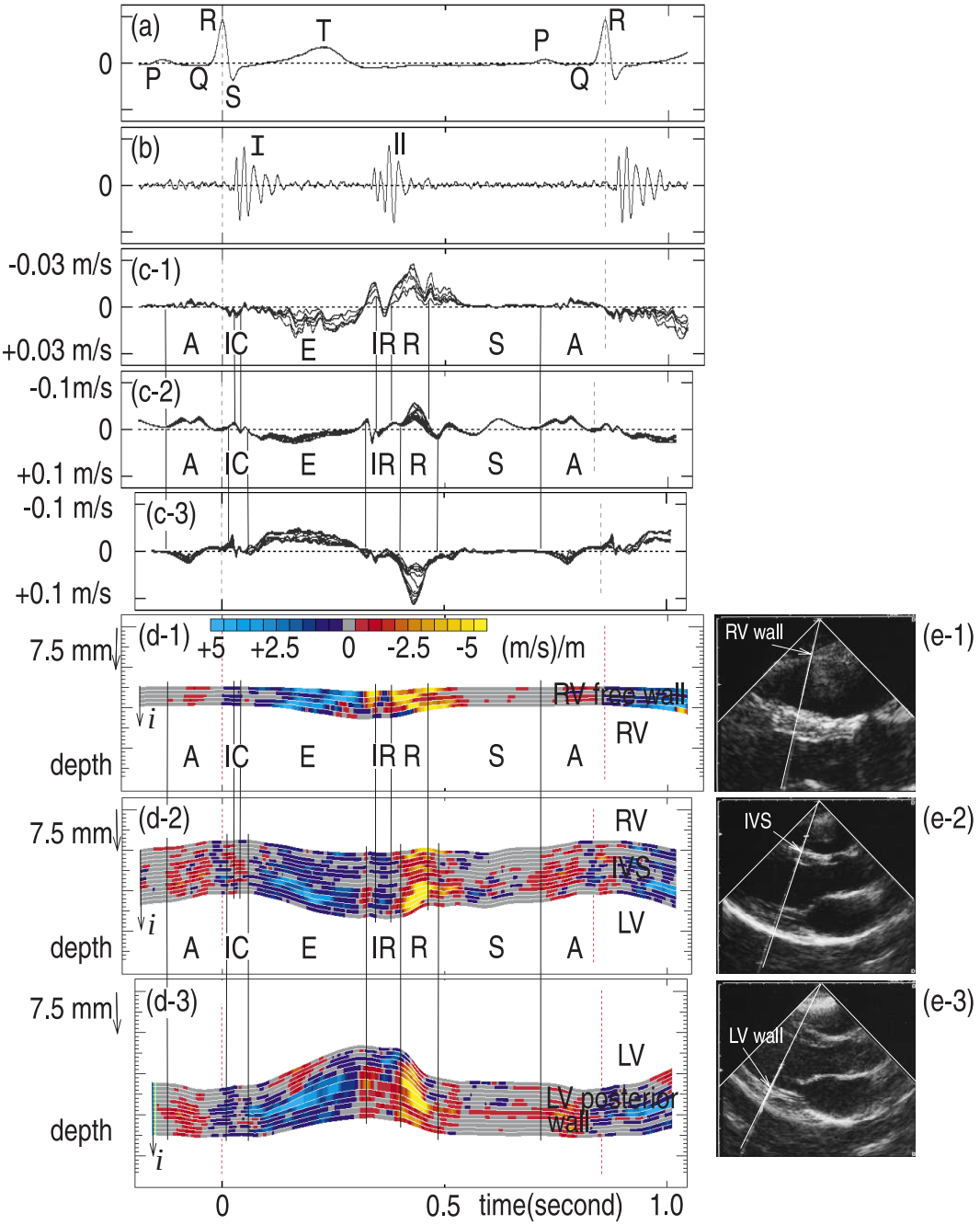

Fig. 2. *In vivo* experimental results on (1) the free wall of the RV, (2) the IVS, and (3) the posterior wall of the LV of a healthy 24-year-old male volunteer. (a) ECG. (b) PCG. (c) Superimposed estimates of the velocity signals $\{\widehat{v}(x_i;t)\}$ of the multiple points $\{i\}$ in each of the three heart walls. (d) The tracking results $\{\widehat{x}_i(t)\}$ of the multiple points $\{i\}$ are shown by white lines. The normalized speed of the change in thickness, $S_i(t)$ [(m/s)/m], is mapped according to the defined color scheme and is superimposed on the tracking results. (e) The B-mode cross-sectional images and the directions of the ultrasonic beam.

out from the ventricles to the aorta or the pulmonary artery because the semilunar valves are still closed.

From the velocity signals in Figs. 2(c-1), 2(c-2), and 2(c-3), it can be seen that there are some pulsive components in this period in the three heart walls. The free wall of the RV and the IVS move causing the RV to shrink. The posterior wall of the LV has velocity components larger than those in the IVS so that the volume of the LV decreases.

From the blue components in Figs. 2(d-1), 2(d-2), and 2(d-3), the posterior wall of the LV and the IVS become slightly thick just after the Q-wave of the ECG. About 30 ms after this change, just after the R-wave of the ECG, the free wall of the RV also becomes slightly thick. Such movement or the change in thickness cannot be recognized in the standard M-mode images.

3.2.3 Ejection period

See period "E" in Figs. 2(c) and 2(d). In this period, just after the semilunar valves open due to the increase of the inner pressure of the LV and RV, the blood in the LV and RV flows out to the aorta or the pulmonary artery due to the contraction of the ventricles.

From the velocity signals in Figs. 2(c-1), 2(c-2), and 2(c-3), it can be seen that there are velocity components with rather simple waveforms in each wall which correspond to

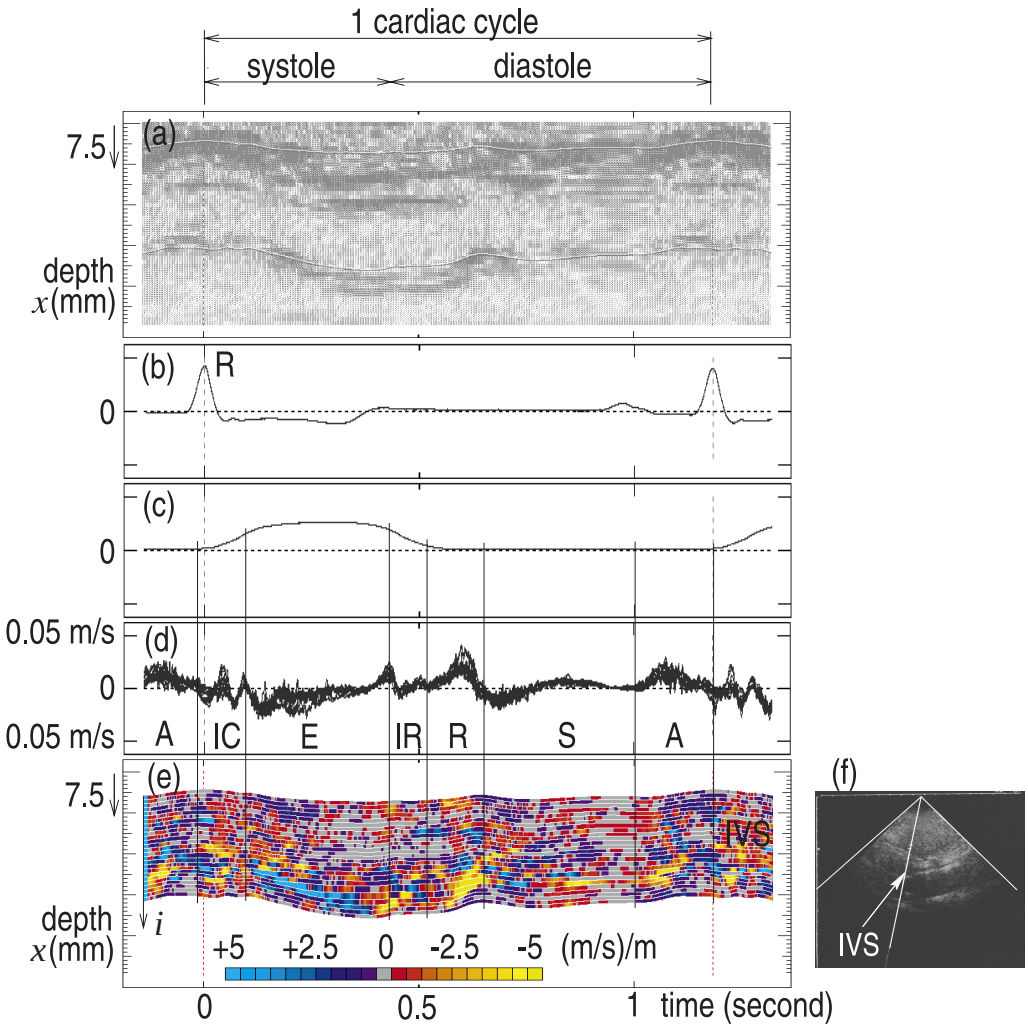

Fig. 3. *In vivo* experimental results on the IVS of a 57-year-old male patient with DCM. (a) M-mode image, (b) ECG. (c) inner pressure of the LV. (d) Superimposed estimates of the velocity signals $\{\hat{v}(x_i\,;t)\}$ of the multiple points $\{i\}$ in the IVS. (e) The tracking results $\{\hat{x}_i(t)\}$ of the multiple points $\{i\}$ are shown by white lines. The normalized speed of the change in thickness, $S_i(t)$ [(m/s)/m], is mapped according to the defined color scheme and is superimposed on the tracking results. (f) The B-mode cross-sectional image and the direction of the ultrasonic beam.

the shrinkage of the RV and the LV.

In this period, there are clear differences in velocity among the layers in each wall, which shows that there is a large change in thickness in each wall. From the blue components in Figs. 2(d-1), 2(d-2), and 2(d-3), it can be seen that there are almost homogeneous changes in thickness in each of the three walls.

3.2.4 Isovolumetric relaxation period

See period "IR" in Figs. 2(c) and 2(d). At the end of the ejection period, the IVS and the posterior wall of the LV have pulsive velocity components with directions opposite those in the previous ejection period indicating that the LV and RV slightly expand and then the inner pressure of the LV and that of the RV become lower than those of the aorta and the pulmonary artery. Therefore, due to these pulsive velocity components, the semilunar valves close at the beginning of this isovolumic relaxation period. Thus, there are rapid decreases (red or yellow components) in the thickness of the free wall of the RV, the IVS, and the posterior wall of the LV as shown in Figs. 2(d-1), 2(d-2), and 2(d-3). However, these components are not clearly recognized in the M-mode image.

Only the pulsive component of the IVS has been previously analyzed in the time domain and the frequency domain,[1,2] and there are clear differences in the power spectra between normals and patients with cardiomyopathy.

At the latter half of this period, the three walls move so that the inner volume of the LV and that of the RV become slowly larger.

3.2.5 Period of rapid filling

See period "R" in Figs. 2(c) and 2(d). In this period, the blood rapidly flows into the LV and the RV. Thus, each wall has large components as shown in Figs. 2(c-1), 2(c-2), and 2(c-3) and there are large differences in velocity among the points in the walls, that is, large changes in thickness in the myocardium. As shown by the red or yellow regions in Figs. 2(d-1), 2(d-2), and 2(d-3), the large decrease in thickness is almost homogeneous in each wall.

3.2.6 Period of slow filling

See period "S" in Figs. 2(c) and 2(d). In the first half of this period, there are phenomena similar to those seen in the previous period of rapid filling.

In the latter half of this period, there is no clear velocity component in the free wall of the RV in Fig. 2(c-1) nor in the posterior wall of the LV in Fig. 2(c-3). There are some

vibration components with a frequency of about 10 Hz in the IVS of Fig. 2(c-2).

Also, there are no remarkable differences between the velocity signals, that is, all points in the three walls move in parallel. Thus, in the latter half of the period, the wall is gray in Fig. 2(d-2).

4. Measurement for a Patient with Dilated-cardiomyopathy

4.1 In vivo experiments and results

As an example of noninvasive diagnosis of the myocardium, we applied the proposed method to the IVS of a 57-year-old male patient with dilated-cardiomyopathy (DCM).

The M-mode image, the ECG, the waveforms of the velocity signals, the normalized speed of change in thickness, $S_i(t)$, and the B-mode image of the IVS are respectively shown in Figs. 3(a), 3(b), 3(d), 3(e), and 3(f). In this measurement, the inner pressure of the LV is simultaneously and invasively measured with catheterization, as shown in Fig. 3(c). From the inner pressure, the boundaries among the six periods described above are largely confirmed.

4.2 Comparison of normal subject with patient

For the healthy subject, the thickness of the IVS is about 10 mm, while for the patient with DCM, the IVS is about 20 mm.

By comparing the velocity signals in Fig. 3(d) with those in Fig. 2(d-2), the envelopes of the waveforms can be seen to be similar.

Comparison of the normalized speed of change in thickness in Fig. 3(e) with that in Fig. 2(d-2) shows that the change in thickness is not homogeneous for the patient. The reason is that the myocardial fibers have complex directions, especially in the half of the IVS next to the RV.

Especially in the period of slow filling, the gray components are not clearly recognized, that is, the myocardium always moves to become thick or thin, even in the diastole.

5. Conclusions

In this paper, we have applied the method developed to the free wall of the RV, the IVS, and the posterior wall of the LV of a healthy young male volunteer and the IVS of a male patient with DCM. From the relationship among the results for the three heart walls and the differences between the subjects, the velocity waveforms and the changes in thickness have been characterized for each period during one cardiac cycle.

In our previous study, detected velocity signals were analyzed in the frequency domain only for the period around the second heart sound emission. The analysis will next be applied to the velocity signals for each of six cardiac periods based on the results presented in this paper.

Further investigation of this proposed method, including its clinical application to the noninvasive local diagnosis of coronary artery disease, drug-induced myocardial disease, and arteriosclerosis of patients including elder subjects, is also being conducted.

Acknowledgements

The authors are grateful to Professor Emeritus Noriyoshi Chubachi of Tohoku University, Professor Kunio Shirato of Tohoku University School of Medicine, and Dr. Yoshiro Uzuka of the Sendai Center for Hematologic Disorders for discussions and encouragement, and Dr. Eiichi Kamata of Tohoku University School of Medicine for helpful discussion and assistance with experiments.

1) H. Kanai, H. Hasegawa, N. Chubachi, Y. Koiwa and M. Tanaka: IEEE Trans. Ultrason. Ferroelectr. & Freq. Control **44** (1997) 752.
2) H. Kanai, M. Sato, Y. Koiwa and N. Chubachi: IEEE Trans. Ultrason. Ferroelectr. & Freq. Control **43** (1996) 791.
3) C. Kasai, K. Namekawa, A. Koyama and R. Omoto: IEEE Trans. Sonics & Ultrason. **32** (1985) 458.
4) A. P. G. Hoeks, C. J. Ruissen, P. Hick and R. S. Reneman: Ultrasound Med. & Biol. **11** (1985) 51.
5) D. E. Hokanson, D. J. Monzersky, S. D. Sumner and D. E. Strandness, Jr.: J. Appl. Physiol. **32** (1972) 728.